NANO LETTERS

pubs.acs.org/NanoLett Letter

Near-Field Thermal Radiation between Two Plates with Sub-10 nm Vacuum Separation

Hakan Salihoglu, Woongsik Nam, Luis Traverso, Mauricio Segovia, Prabhu K. Venuthurumilli, Wen Liu, Yu Wei, Wenjuan Li, and Xianfan Xu*

Cite This: https://dx.doi.org/10.1021/acs.nanolett.0c02137 Read Online

ACCESS | Metrics & More | Article Recommendations | Supporting Information

ABSTRACT: Radiation greatly exceeding blackbody between two objects separated by microscale distances has attracted great interest. However, challenges in reaching such a small separation between two plates have so far prevented studies below a separation distance of about 25 nm. Here, we report a study of radiation enhancement in the near-field regime of less than 10 nm between two parallel plates. We make use of bulk, rigid plates to approach small separation distances without the adverse snap-in effect, develop embedded temperature sensors to allow near-zero separation, and employ advanced sensing method to level the plates and approach and maintain small separations. Our findings agree with theoretical predictions between parallel surfaces with separations down to 7 nm where an 18000 times enhancement in radiation between two quartz plates is observed. Our method can also be used to explore heat transfer between other materials and can possibly be extended to smaller separation gaps.

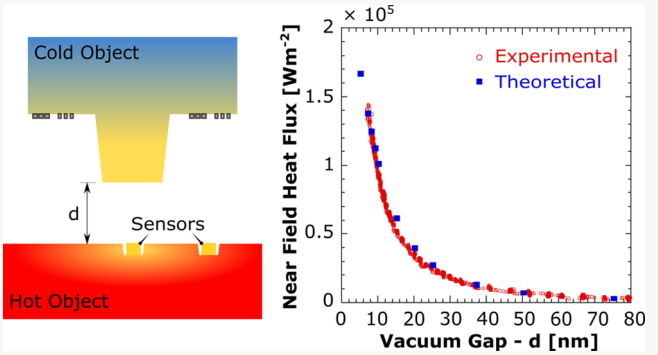

KEYWORDS: *Near-field thermal radiation, parallel plates, nanoscale heat transfer, surface phonon polariton*

Theoretical studies have estimated rapidly increased enhancement in thermal radiative heat transfer between two objects with decreasing separation gap (d) to less than the characteristic radiative wavelength (~10 μm at room temperature) or the near-field.[1−4] To validate near-field radiation enhancement, numerous experimental studies have been conducted. Sophisticated atomic microscopy techniques with specially developed cantilevers have made the measurements possible over a broad range of separation distances, from contact to far-field.[5−10] In contrast, experimental validation for near-field radiation between two parallel plates has inherent complexities in reaching a small separation gap. Earlier experiments have shown the enhancement at a few-micrometer separation distances, which is limited by the lack of control in the parallelism between two bulk surfaces.[11,12] A separation gap in the ~1 μm range was obtained three decades later.[13−15] Investigations at submicrometer gap separation have utilized nanostructured features, such as microscale actuators, nanopillars, or membranes, and sensitive gap measurement techniques.[16−19] Membrane technologies have allowed the observations of near-field enhancement approaching ~50 nm separation, which is limited by contaminations during fabrication and handling, deviation from planar surface as a result of fabrication processing, and challenges in gap control due to snap-in of the membranes.[20,21] Replacing one of the membranes with a bulk, rigid surface has reduced the snap-in and allowed researchers to reach a separation distance of ~25 nm; however, the theoretical predictions at sub-25 nm separation between polar dielectrics remain to be validated.[22]

For practical applications, a substantial amount of near-field radiation will be achieved between two parallel plates instead of between a tip and a plate. Therefore, it is important to investigate near-field radiation between two parallel plates. It is also of great interest to probe near-field radiation between two plates in even closer distances than those have been reported.[20−22] At these closer distances near-field radiation will be dramatically enhanced.[23−25] Here, we develop a comprehensive experimental method to study near-field radiation between two rigid quartz plates with gap separations down to less than 10 nm. We use an interferometric spatial phase imaging (ISPI) system with subnanometer sensitivity to ensure the parallelism of the two plates and to measure and control the gap separation. We also develop microfabricated resistive temperature sensors which are embedded in the substrate to allow close approach of the two surfaces. Our

Received: May 20, 2020
Revised: July 1, 2020
Published: July 6, 2020

https://dx.doi.org/10.1021/acs.nanolett.0c02137
Nano Lett. XXXX, XXX, XXX−XXX

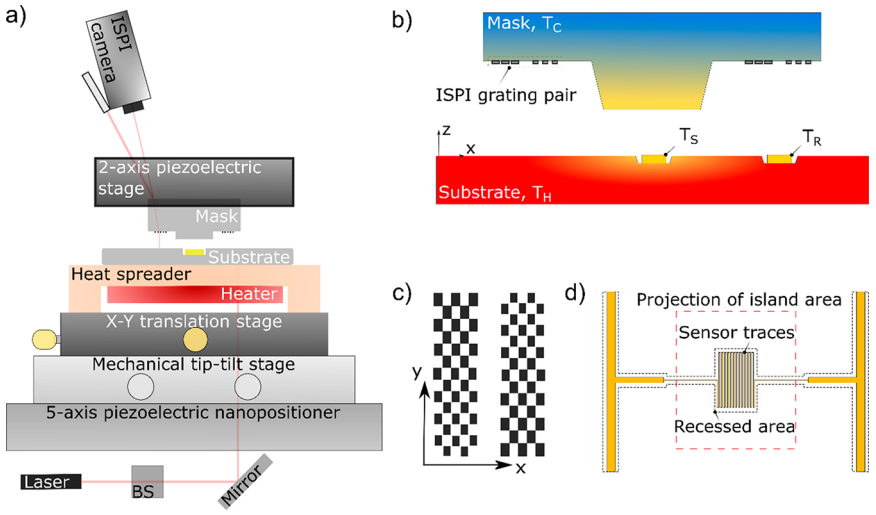

Figure 1. (a) Schematic of the experimental setup. Near-field radiation is measured between the protrusion (or island, 100 μm × 100 μm) on the mask and the substrate, both independently positioned using coarse mechanical translation and tip/tilt stages and piezoelectric stages (2-axis for the mask and 5-axis for the substrate). An optical interferometry system (laser, beamsplitter (BS), and mirror) is used to provide a coarse measurement and alignment of tip-tilt between the mask and the substrate. Interferometric spatial phase imaging (ISPI) is used to provide fine measurement of the tip/tilt and gap size between the mask and the substrate. (b) Close-up views of the mask and the substrate, showing the island on the mask, the grating pairs used for ISPI measurements, and the micro temperature sensors embedded in the substrate. We define bulk temperature of the substrate as T_H and of the mask as T_C. The sensing sensor is at temperature T_S, and the reference sensor is at temperature T_R. A total of eight grating pairs are fabricated to ensure the mask and substrate are parallel. One temperature sensor is positioned directly underneath the island as shown in (d), and the other sensor is used as a reference. (c) Reversely chirped grating pairs for ISPI gap sensing (see Supporting Information 1 for the SEM image). ISPI analyzes diffracted-reflected light from the grating pairs to detect gap separation with a resolution of ~0.2 nm. (d) Top view of the schematic of the temperature sensor and the projected area from the island where there is near-field radiation interaction. The area enclosed in the red dashed line represents the projection area of the island. The black dashed lines around sensor traces denote the recessed region of ~30 nm deep from the substrate surface in which <30 nm tall sensors are fabricated.

results show four orders of magnitude of near-field radiative enhancement compared to the blackbody radiation, and they validate theoretical predictions down to below 10 nm separation. Our experimental technique is promising for investigating near-field radiation between other materials and possibly can be extended to study radiation at even closer separation distances.

Figure 1a shows a schematic overview of the experimental setup and the key components for manipulation of two rigid surfaces (called substrate and mask here), including manual and piezoelectric manipulation stages for both the substrate and the mask, an ISPI (interference spatial phase imaging) system for measuring the gap between the substrate and the mask, an optical interferometry system for coarse tip-tilt measurement, and microfabricated sensors for measuring temperature variation caused by near-field radiation. All the components shown in Figure 1a except the ISPI camera and laser and the optical interferometry components are housed in a vacuum chamber. The entire apparatus is under ultralow-particulate-air (ULPA) filters for sample handling and alignment.

The piezoelectric stages control the relative position and orientation of the substrate and the mask with five and two degrees of freedom, respectively. The large stages in combination with the use of rigid substrates allow the gap between the mask and the substrate to approach zero distance without the adverse snap-in effect until a separation distance of about 1 nm (see below).

An important aspect in our near-field measurement is the control of the nanometer level gap size using an ISPI system. This method was also employed in our previous works for near-field nanolithography[26−28] and near-field nanomaterials growth.[29] To explain briefly, the ISPI method uses interferometric marks consisting of reversely chirped grating pairs (Figure 1c). Illuminated by a laser beam, the grating pairs diffract and reflect the laser beam, forming counter propagating interference patterns that are sensitive to the gap. The phase information of the propagating fringes allows extraction of the gap with a sensitivity of 0.2 nm.[26] A total of eight grating pairs are fabricated on the mask, allowing for leveling the mask with respect to the substrate within 0.03 mrad. Details of the ISPI system are given in Supporting Information 1.

A protrusion, or island, is fabricated on the mask which has an area of about 100 μm × 100 μm and height of about 10 μm (Figure 1b), and near-field radiation is achieved between the surface of this island and the substrate. The use of the relatively small area helps to minimize contaminations during experiments. To induce a temperature difference between the mask and the substrate, a heater is placed underneath the substrate, which heats the substrate through a copper spreader. To detect the temperature variation due to near-field radiation, two identical resistive sensors, called the sensing sensor and reference sensor, are fabricated on the substrate. The sensing sensor, located at the center of the substrate (yellow rectangle in Figure 1a and Figure 1b) and directly underneath the island, undergoes temperature variation with the manipulation of gap distance in the near-field regime. Meanwhile, the reference sensor, which is not underneath the island, provides a reference temperature reading. The mask and the substrate are both made using commercially available bulk substrates, with the mask specially flattened to better than ~80 nm flatness over its length of 12.7 mm. Within the near-field interaction area of 100 μm × 100 μm, it is estimated that the variation of height in this area is less than 1 nm for the mask and ~2 nm for the

https://dx.doi.org/10.1021/acs.nanolett.0c02137
Nano Lett. XXXX, XXX, XXX−XXX

substrate (see Supporting Information 2). A critical feature of the sensors is that they are embedded in the substrate, as shown in Figure 1b and Figure 1d. A recessed area approximately the size of the sensors (36 μm × 45 μm) and the depth of the height of the sensor (30 nm) is made in the substrate first, followed by microfabrication of the sensors (see Supporting Information 2 for fabrication of the mask and the sensors along with the details of the sensors, and see Supporting Information 3 for calibration). The design of the sensors allows the gap between the quartz surface of the mask (island) and the quartz surface of the substrate to approach zero.

Near-field radiation is obtained from differential temperature measurement[30] with the sensing and reference sensors. We raise the substrate temperature to T_H by a constant heat supply from the heater and denote the temperature of the mask as T_C and the difference between the substrate and the mask as ΔT (= $T_H - T_C$). Before the gap between the mask and the substrate approaches the near-field region, the temperature of the sensing sensor (T_S) and the temperature of the reference sensor (T_R) are both at T_H. When the gap approaches the near-field regime, the temperature of the reference sensor remains unchanged ($T_R = T_H$), whereas that of the sensing sensor experiences a variation denoted as ΔT_{NF} (= $T_S - T_R$). The differential circuit scheme enables a measurement sensitivity of ~2 mK (see Supporting Information 3 for calibration of temperature sensors and sensitivity analysis of temperature measurement). We measure this temperature variation arising from the near-field enhancement at different separation gap distances. We then employ a heat transfer model to compute near-field radiative heat flux, q_{NF}, from the substrate ($q_{NF,H}$) to the mask ($q_{NF,C}$) that will give this temperature variation. Details of the heat transfer model is given in Supporting Information 4.

Experiments start with coarse alignment. First, the island is laterally aligned coarsely with respect to the sensing sensor in the camera view. Then, the mask is lowered to a ~150 μm separation gap from ISPI reading, and optical interferometry is used to adjust the parallelism to about 0.1 mrad.[31] Then, fine ISPI alignment is employed by taking ISPI readings from multiple grating pairs to guarantee a parallelism within 0.03 mrad, which corresponds to a 3 nm height difference over the 100 μm length of the island on the mask (see Supporting Information 1). We then provide a fine adjustment of the relative position between the sensor and the island with a precision of a few micrometers, where both are visible in the ISPI camera. We then confirm the parallel alignment between the two plates by observing the sensing temperature variation in response to tip-tilt adjustment (see Supporting Information 1). Once the fine parallel alignment is done to the best of the system's capability, the substrate is retracted and then the gap is gradually reduced to take the temperature readings. Figures 2a–c show ΔT_{NF} in the region of the gap d less than 80 nm, for ΔT (the temperature difference between the substrate and the mask away from the island) of 4.8, 7.1, and 9.8 K, respectively. The experimental measurements show a rapid increase in ΔT_{NF} with the decreasing gap separation. This is particularly notable when the gap is reduced to below ~25 nm.

Figure 2d shows real-time data of gap manipulation (top), ISPI gap reading (middle), and temperature reading (bottom) versus time for the case with ΔT = 7.1 K. As the mask is approaching the substrate using the piezoelectric nanopositioner, the ISPI reading shows the corresponding decrease

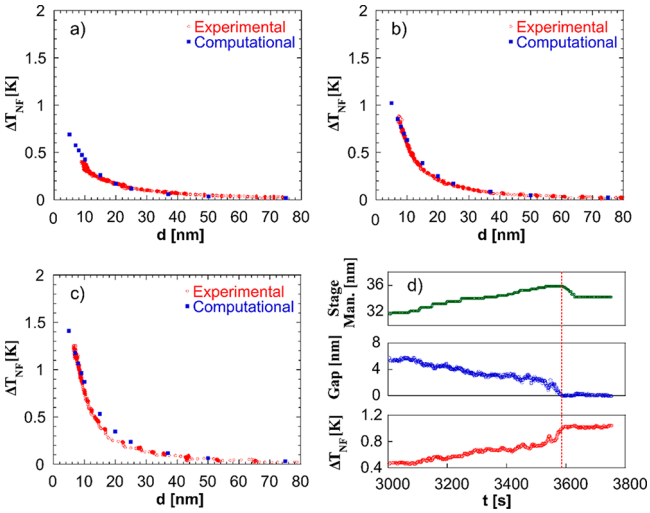

Figure 2. Comparison of measured and computed temperature variation for ΔT (the temperature difference between the substrate and the mask at locations far from the near-field interaction regions) of (a) 4.8 K, (b) 7.1 K, and (c) 9.8 K. Experimental results agree with computations from near-field radiation theory. For the computational results in (a–c), the uncertainty ranges from approximately ±12% at d = 25 nm to approximately ±6% at d = 7 nm (see Supporting Information 4). (d) Real-time approaching data of stage manipulation (top, green), the corresponding ISPI gap reading (middle, blue), and the temperature reading (bottom, red) for ΔT = 7.1 K. The stage reading (top, green) is not absolute. The red dashed vertical line indicates contact. Right before the contact, the ISPI gap reading shows a sudden drop. At the contact, the temperature jumps as well.

in the gap. The decrease in the gap results in temperature change due to near-field radiation (cooling of the surface underneath the island). There is a sudden jump in the ISPI reading and temperature reading at contact in Figure 2d, which lasts over a distance of 1–2 nm. After that, the readings do not change in the time window shown in Figure 2d. The contact point is assigned as 0 gap in the ISPI reading as the ISPI reading is relative (see Supporting Information 1). The red dashed line indicates the time of the contact. We notice that when these sudden changes happen, they cannot be easily reversed even when we try to retract the distance as seen in the top green line in Figure 2d. Larger manipulation (using more than 10 nm input in the piezoelectric nanomanipulator) does break the contact (not shown in figure).

The experimental data ΔT_{NF} in Figures 2a–c are plotted starting from the smallest gap of ~7 nm, which match with the computational results (see below). The reasons for this 7 nm gap can be the combination of the peak-to-peak roughness of the sample surfaces (~2 nm above the surface level of substrate sensing area and <2 nm above that of the island, the RMS roughness is about 1 nm, see Supporting Information 2), the flatness of the samples (<1 nm for the mask and 2 nm for the substrate, see Supporting Information 2), the parallelism achieved between the substrate and the mask (0.02 mrad or 2 nm, as discussed previously), and possibly a jump due to attractive forces at 1–2 nm separation distance (Figure 2d). The last point is also consistent with experimental observation of strong attraction between the mask and the substrate. The collect effects of all the above contribute to the smallest distance of about 7 nm that we can measure the near-field radiation.

https://dx.doi.org/10.1021/acs.nanolett.0c02137
Nano Lett. XXXX, XXX, XXX−XXX

The computed ΔT_{NF} in Figures 2a–c are obtained based on the theoretical heat flux of near-field radiation (see Supporting Information 4 for the computation model). We also show this theoretical near-field heat flux, q_{NF}, computed using fluctuational electrodynamics,[32] in Figure 3a. The experimental heat flux is the heat flux that produces the measured temperature variations shown in Figures 2a–c. The drastic increase in the near-field heat flux is well documented,[4,33,34] due to enhancement in energy transport by surface phonon polaritons excited at near resonance frequencies (see Supporting Information 5 for the theoretical calculation).

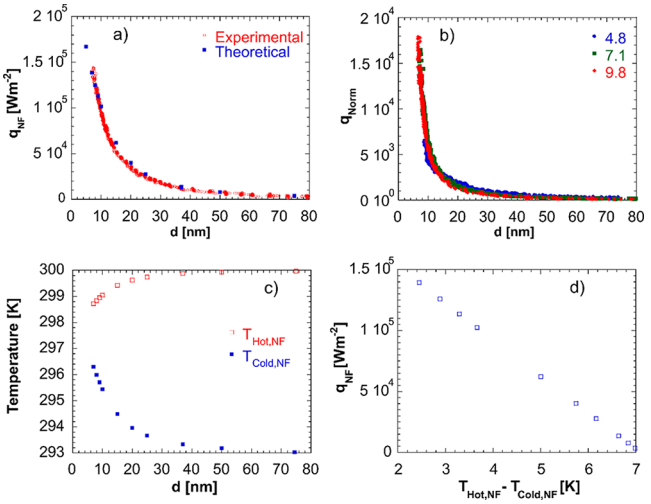

Figure 3. (a) Experimental vs theoretical near-field heat flux vs separation gap for ΔT = 7.1 K. Uncertainty in q_{NF} is approximately ±2% at d = 25 nm and increases with a decreasing gap up to approximately ±9% at d = 7 nm (see Supporting Information 4). (b) Experimental q_{Norm}, the normalized heat flux with respect to blackbody, for all ΔT used. (c) Temperature change over the distance between the two surfaces. $T_{Hot,NF}$ and $T_{Cold,NF}$ represent the temperature of the surface around the sensor on the substrate (hot surface) and the temperature of the island (cold surface), respectively. (d) Near-field radiative heat flux with respect to the temperature difference of the hot and cold surfaces when ΔT = 7.1 K.

To further analyze near-field radiation enhancement, we define a normalized radiative heat flux, q_{Norm}, expressed as ratio of q_{NF} to the far-field radiative heat transfer, q_{FF}, for the same temperature difference. Figure 3b shows q_{Norm} for ΔT = 4.8, 7.1, and 9.8 K. We find that the normalized radiative heat flux overlaps for the three ΔT, indicating the reliability of the experimental results. We calculate a standard deviation of ∼460, ∼700, and ∼90 for a mean of ∼14500, ∼5400, and ∼1530 at 7, 10, and 20 nm gap separations, respectively. The experimental results also agree with theoretical computations down to 7 nm, showing a more than four orders of magnitude enhancement in near-field thermal radiation (q_{Norm} ∼ 18000).

Figure 3c shows the change in temperatures of the hot and cold surfaces exposed to near-field thermal radiation over the distance between the surfaces. The temperature of the hot surface, $T_{Hot,NF}$, cools with the decreasing gap, and the temperature of the cold surface, $T_{Cold,NF}$, heats with the decreasing gap due to near-field heat transfer. We note that, similar to the observation of the notable variation in ΔT_{NF} in Figure 2b, $T_{Hot,NF}$ and $T_{Cold,NF}$ also change significantly below 25 nm. We also notice that the rate of temperature change for the hot surface over the distance is less than that for the cold surface. This arises from the difference in thermal conductivity, where the thermal conductivity of the substrate of the hot surface is greater than that of the mask of the cold surface (see Supporting Information 4 for thermal conductivity). We also show the near-field heat flux as a function of the temperature difference between the hot and cold surfaces ($T_{Hot,NF}$ − $T_{Cold,NF}$) in Figure 3d when ΔT = 7.1 K. Despite the decrease in the temperature difference, the heat flux, q_{NF}, grows approximately linearly with the temperature difference.

Lastly, we anticipate that the experimental technique presented in this work can be used to probe near-field heat transfer between two surfaces at even closer distances. The experiments can be further optimized, for example, by reducing the roughness of the surfaces from processing and using substrates with better flatness. The method can also be extended to study radiative heat transfer between other types of materials such as metasurfaces.

In conclusion, we have developed an experimental technique to measure near-field thermal radiation between two quartz plates separated by a vacuum gap less than 10 nm. Experimental results agree with the theoretical framework and have shown enhancement in near-field radiation between two quartz plates. We have observed more than four orders of magnitude enhancement in thermal radiation at a separation distance of 7 nm. We foresee that this experiment technique is a viable candidate to explore extreme near-field radiation between parallel plates.

■ ASSOCIATED CONTENT

Supporting Information

The Supporting Information is available free of charge at https://pubs.acs.org/doi/10.1021/acs.nanolett.0c02137.

(1) Details of the ISPI measurement; (2) surface characterization of the near-field interaction surfaces on the substrate and the mask; (3) calibration of temperature sensors; (4) computational model along with substrate temperature calibration; and (5) theoretical near-field radiation calculation (PDF)

■ AUTHOR INFORMATION

Corresponding Author

Xianfan Xu − *School of Mechanical Engineering and Birck Nanotechnology Center, Purdue University, West Lafayette, Indiana 47907, United States;* orcid.org/0000-0003-0580-4625; Email: xxu@ecn.purdue.edu

Authors

Hakan Salihoglu − *School of Mechanical Engineering and Birck Nanotechnology Center, Purdue University, West Lafayette, Indiana 47907, United States*

Woongsik Nam − *School of Mechanical Engineering and Birck Nanotechnology Center, Purdue University, West Lafayette, Indiana 47907, United States*

Luis Traverso − *School of Mechanical Engineering and Birck Nanotechnology Center, Purdue University, West Lafayette, Indiana 47907, United States*

Mauricio Segovia − *School of Mechanical Engineering and Birck Nanotechnology Center, Purdue University, West Lafayette, Indiana 47907, United States*

Prabhu K. Venuthurumilli − *School of Mechanical Engineering and Birck Nanotechnology Center, Purdue University, West Lafayette, Indiana 47907, United States*

https://dx.doi.org/10.1021/acs.nanolett.0c02137
Nano Lett. XXXX, XXX, XXX−XXX

Wen Liu − *Center for Micro- and Nanoscale Research and Fabrication, University of Science and Technology of China, Hefei, Anhui 230027, China*
Yu Wei − *Center for Micro- and Nanoscale Research and Fabrication, University of Science and Technology of China, Hefei, Anhui 230027, China*
Wenjuan Li − *Center for Micro- and Nanoscale Research and Fabrication, University of Science and Technology of China, Hefei, Anhui 230027, China*

Complete contact information is available at: https://pubs.acs.org/10.1021/acs.nanolett.0c02137

Author Contributions

X.X. conceived the concept of the work. H.S. developed the near-field radiation experimental setup and procedure and performed the calculations and the experiments as well as the near-field radiation calculation. W.N. designed the sensors. L.T. designed the ISPI mask. W.L., Y.W., W.L., and P.V. fabricated and characterized the substrate and the mask. M.S. conducted the thermal conductivity measurements. The manuscript is written by H.S. and X.X. with comments and inputs from all authors.

Notes

The authors declare no competing financial interest.

■ ACKNOWLEDGMENTS

H.S. acknowledges support from the Ministry of National Education, Turkey. Support of this work by the National Science Foundation (CBET-1804377) is gratefully acknowledged. The authors would like to thank Prof. S. Shen for discussions of the project.

■ REFERENCES

(1) Polder, D.; Van Hove, M. Theory of Radiative Heat Transfer between Closely Spaced Bodies. *Phys. Rev. B* **1971**, *4* (10), 3303.
(2) Loomis, J. J.; Maris, H. J. Theory of Heat Transfer by Evanescent Electromagnetic Waves. *Phys. Rev. B: Condens. Matter Mater. Phys.* **1994**, *50* (24), 18517.
(3) Pendry, J. Radiative Exchange of Heat between Nanostructures. *J. Phys.: Condens. Matter* **1999**, *11*, 6621−6633.
(4) Joulain, K.; Mulet, J.-P.; Marquier, F.; Carminati, R.; Greffet, J.-J. Surface Electromagnetic Waves Thermally Excited: Radiative Heat Transfer, Coherence Properties and Casimir Forces Revisited in the near Field. *Surf. Sci. Rep.* **2005**, *57*, 59−112.
(5) Kittel, A.; Müller-Hirsch, W.; Parisi, J.; Biehs, S.-A.; Reddig, D.; Holthaus, M. Near-Field Heat Transfer in a Scanning Thermal Microscope. *Phys. Rev. Lett.* **2005**, *95*, 224301.
(6) Rousseau, E.; Siria, A.; Jourdan, G.; Volz, S.; Comin, F.; Chevrier, J.; Greffet, J.-J. Radiative Heat Transfer at the Nanoscale. *Nat. Photonics* **2009**, *3*, 514−517.
(7) Shen, S.; Narayanaswamy, A.; Chen, G. Surface Phonon Polaritons Mediated Energy Transfer between Nanoscale Gaps. *Nano Lett.* **2009**, *9* (8), 2909−2913.
(8) Kim, K.; Song, B.; Fernández-Hurtado, V.; Lee, W.; Jeong, W.; Cui, L.; Thompson, D.; Feist, J.; Reid, M. T. H.; García-Vidal, F. J.; Cuevas, J. C.; Meyhofer, E.; Reddy, P. Radiative Heat Transfer in the Extreme near Field. *Nature* **2015**, *528*, 387.
(9) Cui, L.; Jeong, W.; Fernández-Hurtado, V.; Feist, J.; García-Vidal, F. J.; Cuevas, J. C.; Meyhofer, E.; Reddy, P. Study of Radiative Heat Transfer in Ångström- and Nanometre-Sized Gaps. *Nat. Commun.* **2017**, *8*, 14479.
(10) Kloppstech, K.; Könne, N.; Biehs, S.-A.; Rodriguez, A. W.; Worbes, L.; Hellmann, D.; Kittel, A. Giant Heat Transfer in the Crossover Regime between Conduction and Radiation. *Nat. Commun.* **2017**, *8*, 8.
(11) Hargreaves, C. M. Anomalous Radiative Transfer between Closely-Spaced Bodies. *Phys. Lett. A* **1969**, *30A* (9), 491.
(12) Domoto, G. A.; Boehm, R. F.; Tien, C. L. Experimental Investigation of Radiative Transfer Between Metallic Surfaces at Cryogenic Temperatures. *J. Heat Transfer* **1970**, *92* (3), 412−416.
(13) Hu, L.; Narayanaswamy, A.; Chen, X.; Chen, G. Near-Field Thermal Radiation between Two Closely Spaced Glass Plates Exceeding Planck's Blackbody Radiation Law. *Appl. Phys. Lett.* **2008**, *92*, 133106.
(14) Ottens, R. S.; Quetschke, V.; Wise, S.; Alemi, A. A.; Lundock, R.; Mueller, G.; Reitze, D. H.; Tanner, D. B.; Whiting, B. F. Near-Field Radiative Heat Transfer between Macroscopic Planar Surfaces. *Phys. Rev. Lett.* **2011**, *107*, 014301.
(15) Kralik, T.; Hanzelka, P.; Zobac, M.; Musilova, V.; Fort, T.; Horak, M. Strong Near-Field Enhancement of Radiative Heat Transfer between Metallic Surfaces. *Phys. Rev. Lett.* **2012**, *109*, 224302.
(16) St-Gelais, R.; Guha, B.; Zhu, L.; Fan, S.; Lipson, M. Demonstration of Strong Near-Field Radiative Heat Transfer between Integrated Nanostructures. *Nano Lett.* **2014**, *14*, 6971−6975.
(17) Bernardi, M. P.; Milovich, D.; Francoeur, M. Radiative Heat Transfer Exceeding the Blackbody Limit between Macroscale Planar Surfaces Separated by a Nanosize Vacuum Gap. *Nat. Commun.* **2016**, *7*, 12900.
(18) Watjen, J. I.; Zhao, B.; Zhang, Z. M. Near-Field Radiative Heat Transfer between Doped-Si Parallel Plates Separated by a Spacing down to 200 nm. *Appl. Phys. Lett.* **2016**, *109*, 203112.
(19) Desutter, J.; Tang, L.; Francoeur, M. A Near-Field Radiative Heat Transfer Device. *Nat. Nanotechnol.* **2019**, *14*, 751−755.
(20) Song, B.; Thompson, D.; Fiorino, A.; Ganjeh, Y.; Reddy, P.; Meyhofer, E. Radiative Heat Conductances between Dielectric and Metallic Parallel Plates with Nanoscale Gaps. *Nat. Nanotechnol.* **2016**, *11*, 509−514.
(21) St-Gelais, R.; Zhu, L.; Fan, S.; Lipson, M. Near-Field Radiative Heat Transfer between Parallel Structures in the Deep Subwavelength Regime. *Nat. Nanotechnol.* **2016**, *11*, 515−519.
(22) Fiorino, A.; Thompson, D.; Zhu, L.; Song, B.; Reddy, P.; Meyhofer, E. Giant Enhancement in Radiative Heat Transfer in Sub-30 nm Gaps of Plane Parallel Surfaces. *Nano Lett.* **2018**, *18* (6), 3711−3715.
(23) Budaev, B. V.; Bogy, D. B. On the Role of Acoustic Waves (Phonons) in Equilibrium Heat Exchange across a Vacuum Gap. *Appl. Phys. Lett.* **2011**, *99*, 053109.
(24) Sellan, D. P.; Landry, E. S.; Sasihithlu, K.; Narayanaswamy, A.; McGaughey, A. J. H.; Amon, C. H. Phonon Transport across a Vacuum Gap. *Phys. Rev. B: Condens. Matter Mater. Phys.* **2012**, *85* (2), 024118.
(25) Pendry, J.; Sasihithlu, K.; Craster, R. V. Phonon-Assisted Heat Transfer between Vacuum-Separated Surfaces. *Phys. Rev. B: Condens. Matter Mater. Phys.* **2016**, *94*, 75414.
(26) Wen, X.; Traverso, L. M.; Srisungsitthisunti, P.; Xu, X.; Moon, E. E. High Precision Dynamic Alignment and Gap Control for Optical Near-Field Nanolithography. *J. Vac. Sci. Technol., B: Nanotechnol. Microelectron.: Mater., Process., Meas., Phenom.* **2013**, *31* (4), 041601.
(27) Wen, X.; Traverso, M. L.; Srisungsitthisunti, P.; Xu, X.; Moon, E. E. Optical Nanolithography with (/15 Resolution Using Bowtie Aperture Array. *Appl. Phys. A: Mater. Sci. Process.* **2014**, *117*, 307−311.
(28) Wen, X.; Datta, A.; Traverso, L. M.; Pan, L.; Xu, X.; Moon, E. E. High Throughput Optical Lithography by Scanning a Massive Array of Bowtie Aperture Antennas at Near-Field. *Sci. Rep.* **2015**, *5*, 16192.
(29) Srisungsitthisunti, P.; Moon, E. E.; Tansarawiput, C.; Zhang, H.; Qi, M.; Xu, X. Nanometer-Level Alignment Using Interferometric-Spatial-Phase-Imaging (ISPI) during Silicon Nanowire Growth. *Proc. SPIE* **2010**, *7767*, 776707.
(30) Sadat, S.; Meyhofer, E.; Reddy, P. High Resolution Resistive Thermometry for Micro/Nanoscale Measurements. *Rev. Sci. Instrum.* **2012**, *83*, 084902.

(31) Uppuluri, S. M. V.; Kinzel, E. C.; Li, Y.; Xu, X. Parallel Optical Nanolithography Using Nanoscale Bowtie Aperture Array. *Opt. Express* **2010**, *18* (7), 7369.
(32) Biehs, S.-A.; Rousseau, E.; Greffet, J.-J. Mesoscopic Description of Radiative Heat Transfer at the Nanoscale. *Phys. Rev. Lett.* **2010**, *105* (23), 234301.
(33) Mulet, J.-P.; Joulain, K.; Carminati, R.; Greffet, J.-J. Enhanced Radiative Heat Transfer at Nanometric Distances. *Microscale Thermophys. Eng.* **2002**, *6* (3), 209−222.
(34) Rousseau, E.; Laroche, M.; Greffet, J.-J. Asymptotic Expressions Describing Radiative Heat Transfer between Polar Materials from the Far-Field Regime to the Nanoscale Regime. *J. Appl. Phys.* **2012**, *111* (1), 014311.

https://dx.doi.org/10.1021/acs.nanolett.0c02137
Nano Lett. XXXX, XXX, XXX−XXX